Kinetochore-driven outgrowth of microtubules is a central contributor to kinetochore fiber maturation in crane-fly spermatocytes

James R. LaFountain, Jr.[a] and Rudolf Oldenbourg[b,c]
[a]Department of Biological Sciences, University at Buffalo, Buffalo, NY 14260; [b]Cellular Dynamics Program, Marine Biological Laboratory, Woods Hole, MA 02543; [c]Physics Department, Brown University, Providence, RI 02912

ABSTRACT **We use liquid crystal polarized light imaging to record the life histories of single kinetochore (K-) fibers in living crane-fly spermatocytes, from their origins as nascent K-fibers in early prometaphase to their fully matured form at metaphase, just before anaphase onset. Increased image brightness due to increased retardance reveals where microtubules are added during K-fiber formation. Analysis of experimentally generated bipolar spindles with only one centrosome, as well as of regular, bicentrosomal spindles, reveals that microtubule addition occurs at the kinetochore-proximal ends of K-fibers, and added polymer expands poleward, giving rise to the robust K-fibers of metaphase cells. These results are not compatible with a model for K-fiber formation in which microtubules are added to nascent fibers solely by repetitive "search and capture" of centrosomal microtubule plus ends. Our interpretation is that capture of centrosomal microtubules—when deployed—is limited to early stages in establishment of nascent K-fibers, which then mature through kinetochore-driven outgrowth. When kinetochore capture of centrosomal microtubules is not used, the polar ends of K-fibers grow outward from their kinetochores and usually converge to make a centrosome-free pole.**

Monitoring Editor
Kerry S. Bloom
University of North Carolina

Received: Jan 6, 2014
Revised: Feb 20, 2014
Accepted: Feb 20, 2014

INTRODUCTION

For mitosis or meiosis in animal cells, the two asters positioned next to the prophase nucleus generate radial arrays of microtubules. At the core of each aster is a centrosome, consisting of centrioles and surrounding pericentriolar material that assembles the astral arrays of centrosomal microtubules. Centrosomal microtubules have been implicated in the formation of the kinetochore (K-) fibers that connect chromosomes to the spindle poles, specifically via a "search and capture" model (Kirschner and Mitchison, 1986). This model contends that when a dynamic centrosomal microtubule and an unattached kinetochore interact, the microtubule is captured and selectively stabilized, resulting in establishment of a kinetochore microtubule. Search and capture deservedly merits attention because of the way it couples together the formation of K-fibers with their focusing at the spindle poles. Moreover, microtubule capture by kinetochores has been directly observed (Rieder and Alexander, 1990) as a step in formation of K-fibers (for review see Tanaka, 2012). However, although it is commonly stated or implied that the mature K-fibers are generated by repetitive capture of centrosomal microtubules, there is no direct evidence that K-fiber maturation follows that plan.

Centrosome-independent formation of K-fiber microtubules is supported by earlier studies that showed nucleation of microtubules at or near kinetochores during recovery from microtubule assembly arrest (for most relevant work, see Czaban and Forer, 1985), as well as more recently by observations of K-fiber formation on kinetochores in several settings that make the capture of centrosomal microtubules improbable and resulted in formation of K-fibers that were not directed toward a pole. These settings included 1) the anastral side of drug-induced monopolar spindles (Khodjakov *et al.*,

This article was published online ahead of print in MBoC in Press (http://www.molbiolcell.org/cgi/doi/10.1091/mbc.E14-01-0008) on February 26, 2014.

Address correspondence to: James R. LaFountain (jrl@buffalo.edu).

Abbreviations used: K-fiber, kinetochore fiber; LC-PolScope, liquid crystal polarized light microscope; ROI, region of interest.

2003), 2) half-spindles in which one or both centrosomes had been ablated at prophase (Khodjakov *et al*., 2000), and 3) kinetochores that happened to be shielded from or faced away from centrosomes in normal *Drosophila* tissue culture cells (Maiato *et al*., 2004). An insightful hypothesis put forth by Maiato *et al*. (2004) is that formation of K-fibers involves addition of at least some K-fiber microtubules via a kinetochore-driven mechanism not dependent on centrosomes, consisting instead, perhaps, of kinetochore capture of plus ends of short microtubules that are nucleated in the kinetochore's region and provide "seeds" that undergo further growth to form a K-fiber.

Here we examine and find support for the hypothesis of Maiato *et al*. (2004) in a different system, crane-fly spermatocytes, which are well known for their unusually clear birefringent K-fibers at metaphase of meiosis I. We performed a time-lapse imaging study of the life histories of K-fibers with the LC-PolScope, which enables visualizing birefringent microtubules in their "natural' states, without the use of conjugated fluorophores, such as green fluorescent protein. The LC-PolScope acquires images that can be analyzed quantitatively based on the direct correlation between image brightness and magnitude of retardance, which reports the density of microtubules irrespective of their orientation, under near-physiological conditions. With this technique, the number of microtubules per K-fiber cross section, as well as the numbers of microtubules at different points along the length of a K-fiber, can be quantified directly from images of living cells. We employ a strategy analogous to those of Maiato *et al*. (2004) and Khodjakov *et al*. (2003) in our use of cells that had bipolar spindles with a centrosome at only one of their two poles, and then we extend the analysis to normally bicentrosomal spindles.

RESULTS

Flattening of spermatocytes causes random displacement of centrosomes

We intentionally flattened spermatocytes by aspiration of surrounding testicular fluid when making standard oil-coverslip preparations for microscopy (see *Materials and Methods*). Shear forces resulting from aspiration sometimes cause random intracellular rearrangements, including displacement of one of the centrosomes from its normal position near the edge of the nucleus at diakinesis (Figure 1). Although in some cells, displaced centrosomes can reassociate with the spindle (Dietz, 1966), this did not occur in any of the cells presented here.

Flattened spermatocytes create excellent optical conditions for imaging, with all chromosomes usually placed in the same focal plane. In this study, we concentrate on K-fibers of the three autosomal bivalent chromosomes during meiosis I. The two small univalent sex chromosomes exhibit unusual behavior during meiosis I: anaphase lagging, distance segregation, and an attachment to K-fibers obscured by bundles of densely packed, laterally associated microtubules (Steffen, 1986). On the basis of these complications, we chose not to include them here and restrict our attention to the standard, autosomal bivalents.

With regard to displaced centrosomes, questions regarding whether residual pericentriolar material may have remained at predisplacement loci were addressed by Steffen *et al*. (1986), who reported that no such material was found.

Half-spindles lacking a polar centrosome are of normal morphology and are functional

With LC-PolScope imaging, we produced time-lapse movies of spindle morphogenesis in selected highly flattened cells that had a displaced centrosome. Centrosome displacement was readily confirmed based on the birefringence of its astral microtubules evident at diakinesis and then later throughout the course of meiosis I (Figures 1 and 2). All spindles in the five cells we studied remained monocentrosomal throughout the course of meiosis I. The displaced centrosome was well distant from the spindle and did not participate in spindle morphogenesis.

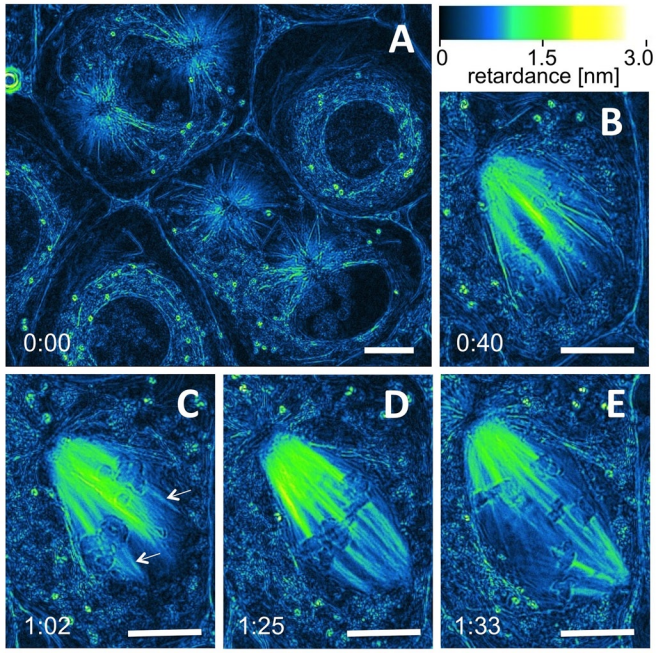

FIGURE 1: LC-PolScope images of flattened spermatocytes, colorized by ImageJ lookup table "green fire blue" (see the text). (A) Wide-field view of two spermatocytes at diakinesis. Top, two centrosomes properly positioned on opposite poles of the nucleus; bottom, one displaced centrosome and one with a normal position next to the nucleus. (B–E) Selected time-lapse images: (B) just after NEB, (C) when nascent K-fibers (arrows) are evident in the centrosome-free half-spindle at angles similar to centrosomal microtubules from the opposite half-spindle, (D) at metaphase showing the disparity in K-fiber retardance in the centrosome-free and centrosomal half-spindles, and (E) mid anaphase A. For time-lapse movie, see Supplemental Movie S1. Time, hours:minutes. Bar, 10 μm.

Color contrast in LC-PolScope images was achieved by applying the ImageJ "green fire blue" lookup table to our retardance black and white LC-PolScope images. Note that in regard to K-fiber retardance at early prometaphase (Figure 1 and Supplemental Movie S1), blue contrast indicates low-level retardance (few microtubules). Subsequently, as a K-fiber matures, its green color indicates increased retardance, and then yellow indicates retardance approaching the 3-nm ceiling. K-fibers reach maximal retardance and maximal microtubules per fiber at metaphase (Figures 1D and 2B), just before onset of anaphase A.

In monocentrosomal bipolar spindles, distinct, nascent K-fibers were evident in the centrosomal half-spindle beginning 20–40 min after nuclear envelope breakdown (NEB). In contrast, in the centrosome-free half-spindles, nascent K-fibers were not evident until ~50–60 min after NEB. In the centrosome-free half-spindle, K-fibers first appeared as short, pointed stubs that grew longer with time to eventually mature to a length similar to that of the K-fibers in the centrosomal half-spindle. K-fiber trajectories in the centrosome-free half-spindle were not initially focused to a pole; instead, they fanned

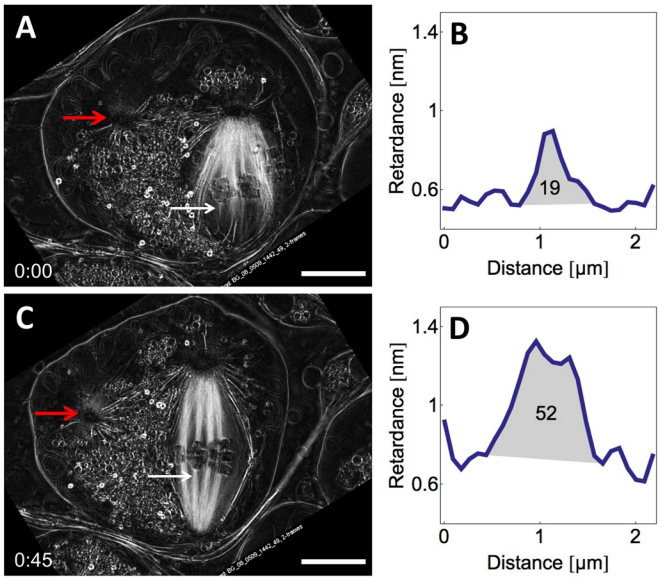

FIGURE 2: LC-PolScope images of a flattened spermatocyte presented as black and white retardance images. (A) Prometaphase when nascent K-fibers are first evident in the centrosome-free half-spindle; red arrow locates the displaced centrosome. (B) Retardance area of nascent K-fiber at the plane pointed out with white arrow is equivalent to 19 microtubules. (C) LC-PolScope image at metaphase; retardance area measured at the plane of the white arrow. (D) Plot profile of plane in C is equivalent to 52 microtubules. For time-lapse movie, see Supplemental Movie S2. Time, hours:minutes. Bar, 10 μm.

out relative to one another, each extending along the same line as the K-fiber from the bivalent's homologous partner to the centrosomal half-spindle. By metaphase, however, the fanned-out poleward ends of the bivalent K-fibers in the centrosome-free half-spindle eventually came together to form a well-focused pole, and the two half-spindles appeared essentially symmetrical.

Thus, somehow, in what must surely be a key element of spindle formation, the microtubule bundles emanating from kinetochores laterally associated at their remote ends as they elongated so as to make a spindle pole. This is consistent with results from Khodjakov *et al*. (2000), who used laser microsurgery to ablate one or both of the centrosomes in cultured fibroblasts and proposed roles for both cytoplasmic dynein and NuMA in focusing K-fibers at centrosome-free spindle poles.

K-fibers grow out from kinetochores in centrosome-free half-spindles

Our quantitative analysis of K-fiber growth in centrosome-free half-spindle produced two important results. First, our "retardance area" algorithm (see *Materials and Methods*) enabled determination of the number of microtubules in a K-fiber. This approach confirmed that as nascent fibers grew longer, they also gained microtubules (Figure 2).

Second, analysis of K-fiber retardance in centrosome-free half-spindles showed that the increases in microtubule number during outgrowth were made at the *kinetochore* end of the fiber (Figure 3 and Supplemental Movie S2). This is evident in the family of curves presented in Figure 3, where the nascent fiber appears as a short stub at time 00:00 (Figure 3A), and then 16 min later (Figure 3B), the fiber clearly had grown longer, with a sizable increase in retardance (due to an increase in microtubule number) at its kinetochore end.

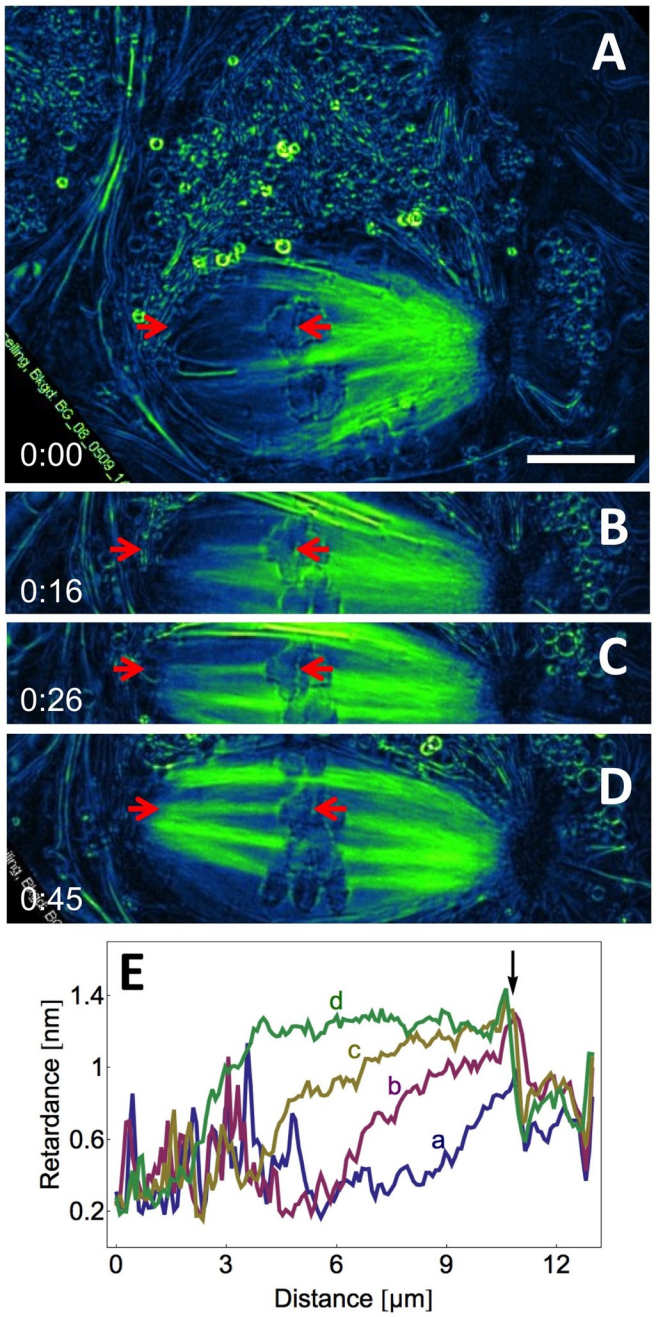

FIGURE 3: K-fiber maturation in a centrosome-free half-spindle. (A–D) LC-PolScope images at different times during maturation with nascent fiber on top and mature metaphase fiber on the bottom. (A) Nascent K-fiber at early prometaphase. (B, C) Elongation of nascent fiber during progression from prometaphase to metaphase. (D) Mature K-fiber at metaphase. Profiles of retardance magnitude along the length of K-fiber were obtained by positioning a 5 × 150 pixel ROI over the fiber of interest and then using the Image J <plot profile> command to generate a curve of retardance magnitude as a function of distance. Red arrows are positioned at the approximate left and right margins of the ROI. (E) Retardance magnitude plots; the black arrow locates the retardance peaks at kinetochores (presumed to be due to edge birefringence and not directly related to microtubules). (a) Profile from A; (b) profile from B; (c) profile from C; (d) profile from D. Maximal retardance poleward away from kinetochores increases with time, as does the magnitude of retardance along the length of a fiber, both interpreted to be a consequence of kinetochore-driven outgrowth of microtubules from the kinetochore. Time, hours:minutes. Bar, 10 μm.

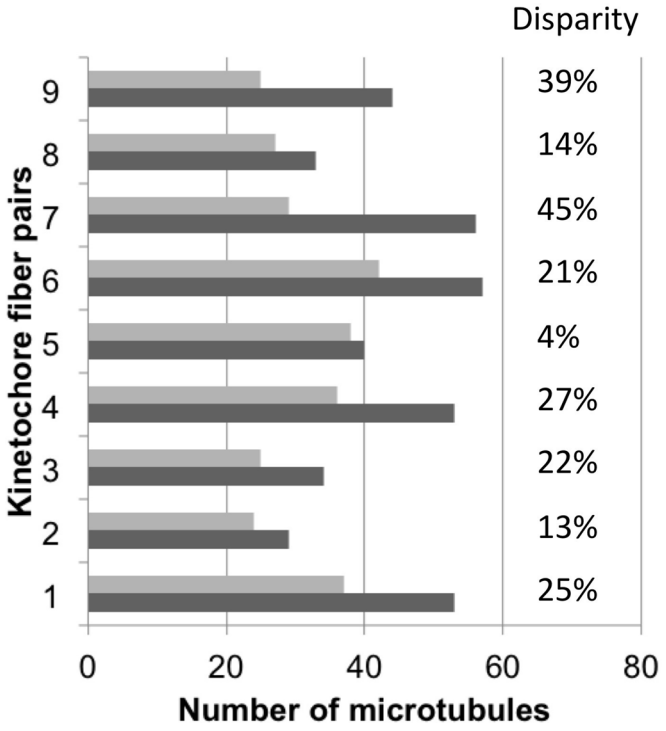

FIGURE 4: Chart of microtubules in pairs of K-fibers from a bivalent to the two poles. Dark bars: from a bivalent to the centrosomal pole; light bars: to the centrosome-free pole. Percentage disparity calculated as in *Materials and Methods*.

Similar increases are evident at later times (Figure 3C), eventually leading to a mature fiber that has a constant high retardance from kinetochore to pole (Figure 3, D, 45 min after A). The retardance along the length of fibers declines by sloping downward toward the pole (Figure 3E), indicating fewer, less densely packed microtubules in the polar region.

Disparity in microtubule content varies among mature partner K-fibers to opposite poles

In cells in which both mature K-fibers of a bivalent could be analyzed, we obtained retardance area measurements on K-fibers to opposite poles: one to the centrosomal pole and the other to the centrosome-free pole. We then used such data to evaluate possible effects of centrosome displacement on the microtubule content of K-fibers. There was a clearly evident pattern in all nine fiber pairs (Figure 4) that were analyzed, in that the less-retardant K-fiber was in the half-spindle that lacked a centrosome. It is true that the range of disparities in Figure 4 (i.e., 4–44%) is within the range of 0–44% found in control cells in an earlier study (LaFountain and Oldenbourg, 2004). Nevertheless, it is significant that in cases reported here the average disparity was 23%, whereas it was only 14% in controls (LaFountain and Oldenbourg, 2004), and as earlier, K-fibers to the centrosome-free pole had the lower retardance. These disparity data suggest that K-fiber retardance is enhanced under centrosomal influence.

In normal cells, nascent K-fibers stand out on a background of centrosomal microtubule arrays

We also examined K-fiber maturation in flattened spermatocytes having properly placed centrosomes. For those cases, nascent fibers first became detectable within the first 10–20 min after NEB. In the most favorable views, in which centrosomal microtubule density was low, weakly retardant fibers (i.e., 10–20 microtubules/fiber) could be detected usually within 10 min post NEB. When nascent fibers took longer (i.e., ~20 min) to be visible over background, there were usually more microtubules per fiber (i.e., 20–30) at the point when they could be detected over background. Hence the range of K-fiber data presented in Table 1 is likely attributable to differences in the degree to which fiber detectability is obscured by background centrosomal microtubules.

LC-PolScope images showed that significant increases in K-fiber retardance were evident during maturation (Figure 5, A and B). Based on such retardance area analysis, the average number of microtubules per K-fiber increased by an average factor of two during the transition from nascent to mature state (Table 1).

	Number of microtubules per K-fiber	
	Range	Average
Spindles with two properly placed centrosomes		
Centrosomal half-spindle		
Nascent	14–34 (n = 9)	24
Mature	29–73 (n = 10)	48
Monocentrosomal spindles		
Centrosomal half-spindle		
Mature	33–57 (n = 6)	47
Centrosome-free half-spindle		
Nascent	8–20 (n = 8)	15
Mature	25–42 (n = 7)	33

Based on retardance area analysis. n is number of K-fibers.

TABLE 1: Nascent and mature kinetochore fibers in centrosomal and centrosome-free half-spindles.

Birefringence increases also occur at kinetochore ends of maturing K-fibers in normal spindles with properly placed centrosomes

Retardance along the length of K-fibers in normal spindles (with properly placed centrosomes) increased in a manner similar to that

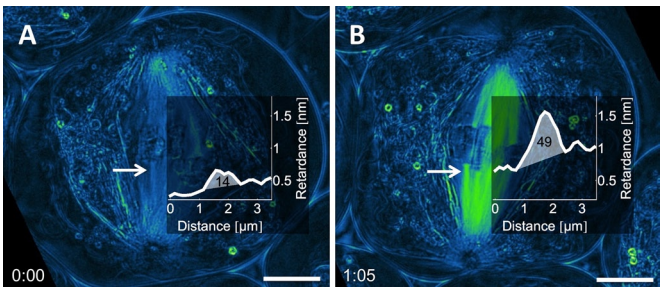

FIGURE 5: K-fibers gain microtubules during maturation. (A) At 18 min after NEB; white arrow locates the plane of a nascent K-fiber that produced the retardance area plot in the inset, an area equivalent to 14 microtubules. (B) At 1 h, 5 min later than A and 3 min before anaphase onset; the retardance of the fiber at the same plane (white arrow) indicates significantly more microtubules, and retardance area (inset) is equivalent to 49 microtubules. Time, hours:minutes. Bar, 10 µm.

in monocentrosomal spindles—namely, increases occurred at the kinetochore ends of K-fibers (Figure 6, A–D, and Supplemental Movie S3) and progressed poleward with time from prometaphase to metaphase (Figure 6E, b–d). By comparison, at the polar ends of their retardance profiles, K-fibers during maturation were essentially unchanged with time (Figure 6E, a–c). In the most mature K-fibers (Figure 6D), the plot of retardance along the fiber shows a clear downslope from the maximal plateau level to a much lower level in the proximity of the centrosome (Figure 6E, d).

Involvement of centrosomal microtubules in nascent K-fiber formation in bicentrosomal spindles

In normal, bicentrosomal spindles, we found that the way a nascent fiber was formed depended on whether or not there was involvement of microtubules from the centrosome to which a kinetochore would eventually be oriented. If this centrosome was distantly located, we found schemes typically similar to that described earlier for K-fibers in centrosome-free half-spindles; that is, the fibers develop as poleward outgrowths from the kinetochore. However, in cells with a proximally located centrosome we found evidence for a mechanism that had features consistent with kinetochore capture of centrosomal microtubules. These two contrasting situations are described in what follows.

An example of the former case is presented in Figure 7 (Supplemental Movie S4, top cell). After NEB, one of the bivalents is positioned near one of the centrosomes but distant from the other. Whereas the nascent fiber to the nearer pole has a *centrosome-directed* trajectory, the nascent fiber to the farther centrosome has a *divergent trajectory* (Figure 7, B–D). Development of such divergent K-fibers proceeds in the same way as we reported for those of centrosome-free half-spindles, that is, through kinetochore-driven outgrowth. The divergent K-fiber grows and moves so that its poleward (minus) end becomes associated with the distant centrosome, and by metaphase its divergence is rectified (Figure 7, E and F). As a result, a spindle with normal morphology is formed. Bipolar orientation of such bivalents and subsequent segregation of their homologues is normal. These findings were noted for nine K-fibers in eight different cells.

In contrast, the scenario of what we interpret to be kinetochore "capture" of centrosomal microtubules is very different (Figure 8, A–C, and Supplemental Movie S5, bottom right cell). We saw this distinctive behavior in 34 bivalents in which one (or both) of its first detectable nascent K-fibers had a trajectory aimed directly at a centrosome.

Just after NEB, the isotropic nuclear space (Figure 8I, a) is penetrated by centrosomal microtubule arrays. These arrays exhibit much greater retardance near the centrosome than at their unattached ends. This must mean that the density of microtubules is highest at the edge of the centrosome and then drops with distance, with fewer microtubules extending farther, distal to the centrosome. Under conditions for best resolution, microtubules of centrosomal arrays are contained in bundles of three to five microtubules. There appear to be no microtubules emanating from kinetochores, based on profiles that show retardance of adjacent unattached bivalents having the same retardance magnitude as isotropic nuclear space before NEB (Figure 8I, b).

Kinetochore capture of centrosomal microtubules occurred within 10 min after NEB, when growth of centrosomal microtubules was taking place (Figure 8, A–C). The time from NEB to first detection of such captured nascent K-fibers was only 6 ± 3 min (n = 34) versus 19 ± 6 min (n = 9) for cases as earlier in which capture of centrosomal microtubules apparently did not occur. At the time

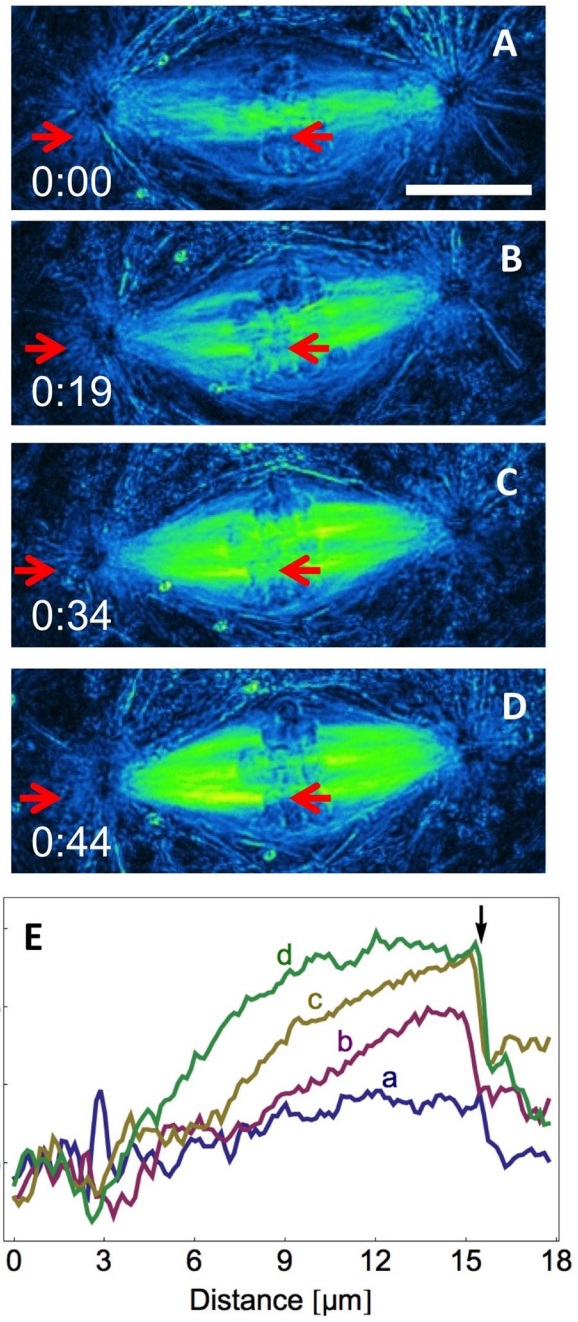

FIGURE 6: Microtubules are added to K-fibers at kinetochore ends in normal spindles. (A–D) LC-PolScope images at different times during maturation; images were rotated to position the K-fiber of interest horizontally. (A) Nascent fiber: red arrows locate the left and right margins of the 5- by 125-pixel ROI that was positioned over each image to generate plots of retardance as a function of distance along the fiber; the right margin of all plots is the plane of cohesion between homologues. (B) Prometaphase nascent fiber gains retardance at kinetochore end. (C) Retardance increases at kinetochore end and spreads poleward. (D) Metaphase showing maximal retardance along the length of the K-fiber and then dropping as fiber approaches the pole. (E) Profiles of retardance magnitude along the length of the K-fiber from each of the images. (a) Profile from A; (b) profile from B; and so on. Black arrow locates positions of kinetochores; retardance increases are at the kinetochore end, and they progress poleward with time along the length of a fiber. Images from Supplemental Movie S3 (left cell). Time, hours:minutes. Bar, 10 μm.

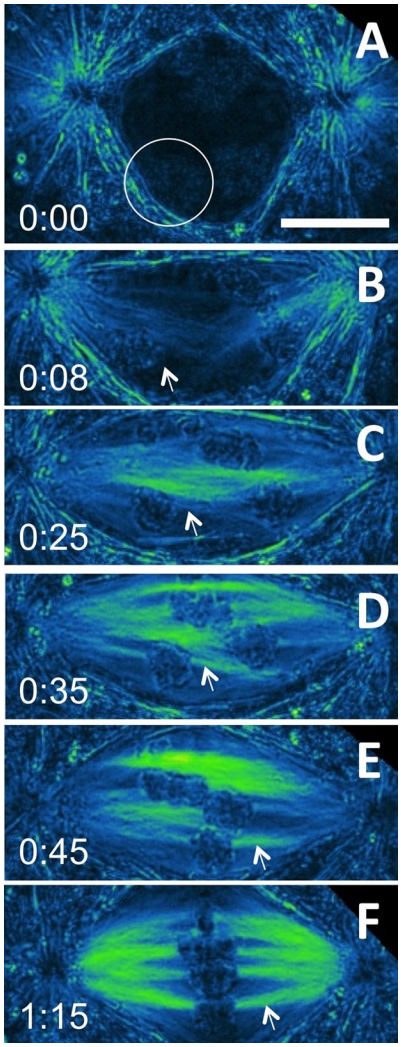

FIGURE 7: Divergent K-fiber growth and attraction of its minus end to a distant centrosome. LC-PolScope images from diakinesis to metaphase I. (A) At diakinesis, the bivalent of interest is encircled at the nuclear periphery, near the nuclear envelope; nuclear space around bivalents appears isotropic. (B) After NEB, centrosomal microtubules invade nuclear space; the region located with the arrow remains isotropic as it was before NEB; there is no evidence of microtubules in this region; bivalent of interest appears to be shielded from the distal centrosome by other bivalents. (C) At ~29 min after NEB, a nascent K-fiber (arrow) is detectable as it grows out with a divergent trajectory, not aimed at the distal centrosome. (D) Further growth and increase in retardance of the divergent K-fiber (arrow) is evident. (E) The trajectory of the divergent K-fiber (arrow) changes as its minus end is attracted to the distal centrosome. (F) Metaphase after the previously divergent K-fiber (arrow) has established normal alignment with respect to the centrosome. Images from Supplemental Movie S4 (upper left cell). Time, hours:minutes. Bar, 10 μm.

of capture, centrosomal microtubules appeared to be the predominant, if not the only, microtubules between chromosomes and centrosomes. The earliest profiles of a captured centrosomal bundle had downward slopes from the centrosome toward the kinetochore (Figure 8I, c), resembling closely the slope of centrosomal microtubules before attachment (Figure 8I, b). Early retardance profiles generated during the first 10 min of prometaphase suggest that the number of microtubules needed to establish a nascent fiber (Figure 8I, c) is quite low—perhaps as few as one or two centrosomal bundles of three to five microtubules each.

With 8 of the 34 fibers that were identified as having been captured, there was centrosome-directed movement of the attaching chromosome at maximal velocities of up to ~2 μm/min (Figure 8, B, C, H, and I, b and c). We cannot be certain whether this movement was due to *end-on* capture of microtubules or *lateral interaction* with microtubules. However, such poleward movement typically was preceded by away-from-the-pole chromosome movement, as if possibly the chromosome had been pushed by growing plus ends of encroaching centrosomal microtubules. Then, after capture, the chromosome moved toward the centrosome.

In the short term, subsequent increases in retardance of a captured K-fiber were evident along its entire length, indicating that microtubule polymer was adding at both centrosomal and kinetochore ends, as well as in between (Figure 8, I, c and d, from C and D, respectively). In the long term, however, kinetochore-driven outgrowth dominates (Figure 8, E and F), eventually generating a mature K-fiber having ~50 microtubules (Figure 8, G and I, g).

DISCUSSION

Toward an understanding of the mechanisms underlying K-fiber morphogenesis

We used time-lapse LC-PolScope imaging to investigate how K-fibers are formed during meiosis I in crane-fly spermatocytes. K-fiber microtubules are birefringent, and that quality enabled direct quantitation of the microtubule content of K-fibers in both space and time. Our objective was to quantify the steps of K-fiber maturation under near-physiological conditions, based on the natural form birefringence of K-fiber microtubules.

LC-PolScope measurements showed that addition of microtubules to maturing K-fibers occurs via kinetochore-driven outgrowth. We studied three different spindle constructs: 1) spindles lacking one centrosome, 2) normal spindles with both centrosomes, and 3) spindles in which one kinetochore of one bivalent lacked access to a distant centrosome. In each case we found that during nascent-to-mature K-fiber progression, addition of microtubules to a K-fiber occurred at its kinetochore-attached end.

Although the endgame of K-fiber maturation seems to be dominated by kinetochore-mediated addition and outgrowth of microtubules, we found that the early stages of K-fiber formation are greatly accelerated by capture of centrosomal microtubules. In spindles with only one centrosome, the half with the centrosome establishes nascent K-fibers much more quickly than the half without centrosome, which only later catches up to contribute to a spindle with nearly symmetric halves.

A mechanism based on kinetochore capture is supported by imaging of nascent K-fibers

At the very early stages of prometaphase, our images provided views of centrosomal microtubules converting to K-fibers, this all occurring at the time of initial kinetochore attachment. Such images of capture are limited to the resolution of the LC-PolScope, and therefore details regarding whether capture entails end-on or lateral kinetochore-with-microtubule attachments have not been discerned. The occurrence of capture is further supported by our observation of capture-related poleward movement.

Two additional findings support kinetochore capture. First, disparities in K-fiber content in the two half-spindles of monocentrosomal spindles were weighted in favor of the centrosomal half of the spindle. We take the view that K-fibers connected to the centrosomal pole have more microtubules because each fiber contains

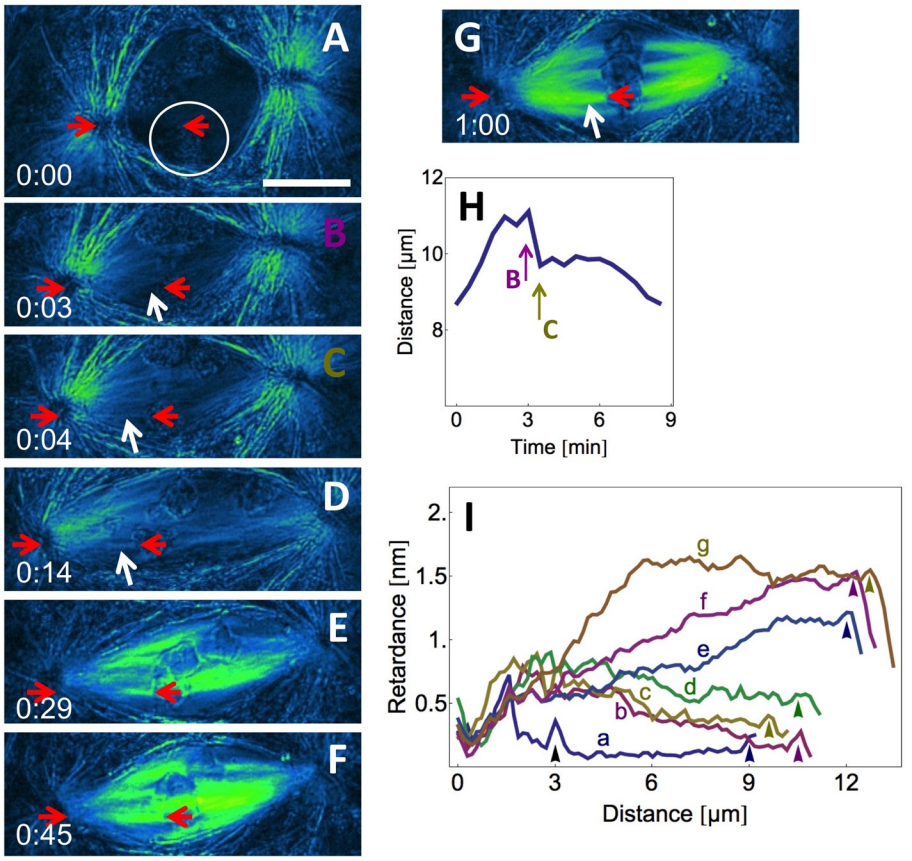

FIGURE 8: (A–F) LC-PolScope evidence for kinetochore capture after NEB. (A) Diakinesis; the bivalent of interest is in the circle. (B) At 2 min after NEB; centrosomal microtubules invade the nuclear space; arrow points to microtubule-free nuclear space between the centrosomal array and the bivalent, which is not yet attached. (C) At 3 min after NEB; the bivalent attaches to the centrosomal bundle and moves toward the pole; nascent K-fiber (arrow) is formed. (D) At 12 min after NEB; the nascent K-fiber is well defined (arrow), as is its partner K-fiber to the opposite pole. (E) Prometaphase: 27 min after NEB; K-fiber maturation is underway, and birefringence increases at the kinetochore end of the K-fiber. (F) Approaching metaphase: 43 min after NEB; further maturation. (G) Metaphase: 61 min after NEB; maximal retardance of K-fiber along its length. (H) Distance (ordinate) vs. time (abscissa) plot after NEB for the captured kinetochore in A–D. Initial movement (before time of magenta arrow) is away from the pole, followed by poleward movement (ending at the gold arrow, as in C). (I) Retardance profiles from A–G. (a) Profile of A in plane indicated by red arrows in A with left margin at the center of the centrosome (location of polar basal bodies) and right margin at the edge of the bivalent of interest (blue arrowhead); black arrowhead locates nuclear envelope. (b) Profile of plane between red arrows in B; kinetochore (magenta arrowhead) at the right margin is not yet attached; note that the retardance magnitude between the chromosome and the plus end of the centrosomal bundle is similar to that of microtubule-free, isotropic nuclear space. (c) Profile of plane between red arrows in C; the kinetochore (gold arrowhead) is attached and has moved poleward (see distance vs. time plot in I). (d) Profile of plane between red arrows in D; the attached kinetochore (green arrowhead) of nascent fiber starts to congress, moving toward the equator. (e) Profile of plane between red arrows in E; magnitude of birefringence at the kinetochore end of the K-fiber increases (blue arrowhead). (f) Profile of plane between red arrows in F; magnitude of birefringence at the kinetochore end of the K-fiber increases further (fuchsia arrowhead). (g) Profile of plane between red arrows in G; magnitude of birefringence is maximal along the length of the K-fiber (gold arrowhead). Images from Supplemental Movie S5 (bottom right cell). Time, hours:minutes. Bar, 10 µm.

both a "nascent" fraction that came from the centrosome and another portion added during maturation by kinetochore-driven outgrowth. Although some disparity between partner K-fibers is normal (LaFountain and Oldenbourg, 2004), we interpret the observed large average disparity as revealing the effect of the absence of capture in centrosome-free half-spindles.

Second, our analysis of nascent K-fibers in regular, bicentrosomal spindles yielded profiles showing incremental increases in retardance along the entire length of K-fibers, as evidenced in Figure 8I, b–d. For such cases, one interpretation is that Figure 8Ic evolved into Figure 8Id by plus-end growth of centrosomal microtubules, followed by capture by the kinetochore. The outcome would be a K-fiber containing additional centrosomal microtubules that were added to those already evident in Figure 8Ic.

Note that LC-PolScope live-cell imaging does not resolve single microtubules, only bundles of at least three to five microtubules. With regard to the classic, end-on capture model proposed by Kirschner and Mitchison (1986), one might speculate that nascent K-fibers are generated as first one centrosomal microtubule is, by chance, captured; then another that happens to adopt the same track as the first; then another; until, finally, an LC-PolScope-detectable bundle is seen. An alternative is that before capture, individual centrosomal microtubules might form with multiple, divergent trajectories; these then associate laterally into bundles; and after they have grown to a substantial length from the centrosome, by chance, a kinetochore "finds" the bundle and connects to it. Other "in-between" alternatives are possible. These are crucial unresolved issues as we move closer to a higher level of understanding of this important stage of meiosis.

During growth of nascent K-fibers, microtubules are added to kinetochore ends

Our observation that kinetochore microtubules were added to kinetochore ends of K-fibers *without* the capturing of centrosomal microtubules lends solid support for the model advocated by Maiato *et al.* (2004), who proposed that growth of microtubules from kinetochores might be universally operative in spindle assembly. This was envisioned not only in situations in which a kinetochore does not have access to a centrosome, but also in normal astral spindles, in which kinetochores may initially capture centrosomal microtubules and then subsequently, as we show, grow by a kinetochore-driven process.

Spermatocytes are capable of generating a full half-spindle that lacks a centrosome at its pole. With our methods, we have not seen a complete bipolar spindle that lacks centrosomes at both poles. This, however, was demonstrated by Khodjakov *et al.* (2000), who used laser microsurgery to eliminate centrosomes from animal cells and found that resulting cells were capable of forming fully competent spindles. Similar findings

achieved via a different approach were also reported by Rebollo *et al*. (2004). All these findings support the view of Wadsworth and Khodjakov (2004), who proposed that there is commonality in the mechanisms of spindle morphogenesis in all plant (acentrosomal) and animal (centrosomal) spindles. Of importance, this commonality does not require the presence of centrosomes or the capture of existing centrosomal microtubules when centrosomes are present. Notable in this regard are recent findings presented by Sir *et al*. (2013), who used a genetic ablation approach to reveal the consequences of loss of centrioles on chromosome segregation in chicken DT40 cells.

With regard to the mechanism underlying the addition of microtubule polymer to kinetochore-attached ends, we propose first in general terms that there is a mechanistic link between, on one hand, nascent-to-mature K-fiber growth and, on the other, earlier-reported (LaFountain *et al*., 2001, 2004) poleward microtubule flux of kinetochore microtubules. To generate an increase in the number of microtubules per K-fiber, Maiato *et al*. (2004) suggested that capture of plus ends of short microtubules nucleated nearby kinetochores provides "seeds" that could then grow by addition of tubulin subunits—of importance to their kinetochore-attached plus ends. That hypothesis of growth based on plus-end addition correlates nicely with our earlier direct visualization of flux (LaFountain *et al*., 2004).

An answer to questions about the nature of such "seeds" emerged after the discovery of augmin-γ-TuRC–mediated branching of microtubules (Goshima *et al*., 2007, 2008). If applicable to spermatocytes, we propose that the plus end of a just-captured daughter microtubule branch could be a seed that anchors to the kinetochore of a nascent K-fiber and then grows poleward by plus-end addition. That daughter microtubule's minus end would remain associated with its also-captured mother microtubule (Kamasaki *et al*., 2013), and both mother and daughter would be expected to be driven poleward by the flux machine (LaFountain *et al*., 2001, 2004). That would be consistent with the proposed link between outgrowth and flux.

Whether augmin-γ-TuRC exists in spermatocyte spindles is one of the questions that remain as challenges for the future. Another is how plus and minus ends of the various spindle microtubules are distributed in the different spindle constructs that were studied. Our data do not speak to that.

Conclusion

Our experimental findings using polarized light microscopy shed light on the microtubule dynamics in K-fibers during stages of meiosis in crane-fly spermatocytes. We identified a period in which the increase of microtubule density in K-fibers clearly originates from the kinetochore. The increased density then elongates toward the pole, possibly (probably) by addition of tubulin at microtubule plus ends anchored in the kinetochore. These mechanisms are active in regular bicentrosomal spindles and in monocentrosomal spindles and lead to nearly equal spindle halves at metaphase in either case.

MATERIALS AND METHODS

Cell culture and cell flattening by microaspiration

Live cell cultures of spermatocytes from the crane-fly, *Nephrotoma suturalis*, were prepared using the standard methodology described in Janicke and LaFountain (1986) and LaFountain and Oldenbourg (2004), which entails spreading cells at an oil/coverglass interface. To achieve the desired degree of cell flattening to aid imaging and cause random displacement of centrosomes, testicular fluid surrounding cells under oil was aspirated with a micropipette prepared beforehand by melting and pulling a glass capillary tube (outside diameter, 1.0 mm; inside diameter, 0.78 mm; length, 10 cm) to the desired bore size (~10–20 μm in diameter). Aspiration was done manually under observation with phase contrast at 100× (10× objective, 10× oculars), until the desired degree of flattening was achieved.

Aspiration attained two goals: 1) it had the effect of flattening the spindle, effecting direct visualization of the full lengths of all (or most) K-fibers in one focal plane from kinetochore to pole (Figure 1), and 2) flattened cells were compressed between the coverslip and overlaid oil, and thus the inherent Brownian "bounciness" evident in preparations of unflattened cells was minimized (but could not be eliminated!). Flattening created a more stable (with negligible movement in and out of focus) object for time-lapse imaging than is possible without it.

Imaging

Imaging of spindle birefringence was done using LC-PolScope workstations described in detail by LaFountain and Oldenbourg (2004) and LaFountain *et al*. (2012). Black and white retardance images were converted to color using the ImageJ (National Institutes of Health, Bethesda, MD) "green fire blue" lookup table. It is important to note that with this color enhancement, blue contrast indicates low retardance above a nonbirefringent (black) background, green color-codes intermediate retardance (higher than indicated by blue), and yellow indicates retardance approaching the 3-nm ceiling set for all images acquired in this study.

Analysis of retardance

The retardance area algorithm is used to make quantitative determinations of the microtubule content of K-fibers. We used this technique in an earlier study (LaFountain and Oldenbourg, 2004), where we describe both the rationale behind it and the way(s) it can be used to "count" microtubules. In practice, its deployment requires that one be able to select K-fibers in sufficient focus that fiber boundaries can be distinguished above background. Here we made such selections by placing a rectangular region of interest (ROI) of 3 by 25 pixels within 1 μm of the kinetochore; the long axis of the rectangle was perpendicular to the fiber axis. The algorithm then calculated the microtubules in the fiber based on the fiber's retardance above the retardance of the background surrounding the fiber.

For profile plots of retardance along the lengths of K-fibers during the course of their maturation, a rectangular ROI of 5 by as many as 150 pixels was positioned with the window of its long axis covering a horizontally positioned K-fiber. This analysis was performed on time-lapse frames taken at successive times during K-fiber maturation and generated plots revealing where new polymer was added during maturation.

For statistical analysis of kinetochore fiber microtubules reported in Figure 4, we used the expression "percentage disparity," which was calculated based on the following common statistical expressions for Average and SD (StdDev):

$$\text{Percentage disparity} = \text{StdDev}(n_1, n_2)/\text{Average}(n_1, n_2)$$

with

$$\text{Average}(n_1, n_2) = (n_1 + n_2)/2$$

$$\text{StdDev}(n_1, n_2) = \text{SQRT}\{[n_1 - \text{Average}(n_1, n_2)]^2 + [n_2 - \text{Average}(n_1, n_2)]^2\}$$

ACKNOWLEDGMENTS

We are most grateful for the constructive input offered by our colleagues Marie A. Janicke and Geoffrey K. Rickards during the course of preparing this article. This work was supported by Grant EB002045 from the National Institute of Biomedical Imaging and Bioengineering awarded to R.O.

REFERENCES

Czaban BB, Forer A (1985). The kinetic polarities of spindle microtubules *in vivo*, in crane-fly spermatocytes. Kinetochore microtubules that re-form after treatment with Colcemid. J Cell Sci 79, 1–37.

Dietz R (1966). The dispensability of the centrioles in the spermatocyte divisions of *Pales ferruginia* (Nematocera). Heredity 19 (Suppl), 161–166.

Goshima G, Mayer M, Zhang N, Stuurman N, Vale RD (2008). Augmin: a protein complex required for centrosome-independent microtubule generation within the spindle. J Cell Biol 181, 421–429.

Goshima G, Wollman R, Goodwin SS, Zhang N, Scholey JM, Vale RD, Stuurman N (2007). Genes required for mitotic spindle assembly in *Drosophila* S2 cells. Science 316, 417–421.

Janicke MA, LaFountain JR Jr (1986). Bivalent orientation and behavior in crane-fly spermatocytes recovering from cold exposure. Cell Motil Cytoskeleton 6, 492–501.

Kamasaki T, O'Toole E, Kita S, Osumi M, Usukura J, McIntosh JR, Goshima G (2013). Augmin-dependent microtubule nucleation at microtubule walls in the spindle. J Cell Biol 202, 125–33.

Khodjakov A, Cole RW, Oakley BR, Rieder CL (2000). Centrosome-independent mitotic spindle formation in vertebrates. Curr Biol 10, 59–67.

Khodjakov A, Copenagle L, Gordon MB, Compton DA, Kapoor TM (2003). Minus-end capture of preformed kinetochore fibers contributes to spindle morphogenesis. J Cell Biol 160, 671–683.

Kirschner M, Mitchison T (1986). Beyond self-assembly: from microtubules to morphogenesis. Cell 45, 329–342.

LaFountain JR Jr, Cohan CS, Oldenbourg R (2012). Pac-man motility of kinetochores unleashed by laser microsurgery. Mol Biol Cell 23, 3133–3142.

LaFountain JR Jr, Cohan CS, Siegel AJ, LaFountain DJ (2004). Direct visualization of microtubule flux during metaphase and anaphase in crane-fly spermatocytes. Mol Biol Cell 15, 5724–5732.

LaFountain JR Jr, Oldenbourg R (2004). Maloriented bivalents have metaphase positions at the spindle equator with more kinetochore microtubules to one pole than to the other. Mol Biol Cell 15, 5346–5355.

LaFountain JR Jr, Oldenbourg R, Cole RW, Rieder CL (2001). Microtubule flux mediates poleward motion of acentric chromosome fragments during meiosis in insect spermatocytes. Mol Biol Cell 12, 4054–4065.

Maiato H, Rieder CL, Khodjakov A (2004). Kinetochore-driven formation of kinetochore fibers contributes to spindle assembly during animal mitosis. J Cell Biol 167, 831–840.

Rebollo E, Llamazares S, Reina J, Gonzalez (2004). Contribution of noncentrosomal microtubules to spindle assembly in *Drosophila* spermatocytes. PLoS Biol 2, E8.

Rieder CL, Alexander SP (1990). Kinetochores are transported poleward along a single astral microtubule during chromosome attachment to the spindle in newt lung cells. J Cell Biol 110, 81–95.

Sir J-H, Pütz M, Daly O, Morrison CG, Dunning M, Kilmartin JV, Gergeley F (2013). Loss of centrioles causes chromosomal instability in vertebrate somatic cells. J Cell Biol 203, 747–756.

Steffen W (1986). Three-dimensional architecture of chromosomal fibres in the crane fly: co-oriented autosomal bivalents and amphitelic sex univalent during prometaphase. Chromosoma 94, 107–114.

Steffen W, Fuge H, Dietz R, Bastmeyer M, Müller G (1986). Aster-free spindle poles in insect spermatocytes: evidence for chromosome-induced spindle formation? J Cell Biol 102, 1679–1687.

Tanaka K (2012). Dynamic regulation of kinetochore-microtubule interaction during mitosis. J Biochem 152, 415–424.

Wadsworth P, Khodjakov A (2004). *E pluribus unum*: towards a universal mechanism for spindle assembly. Trends in Cell Biol 14, 413–419.